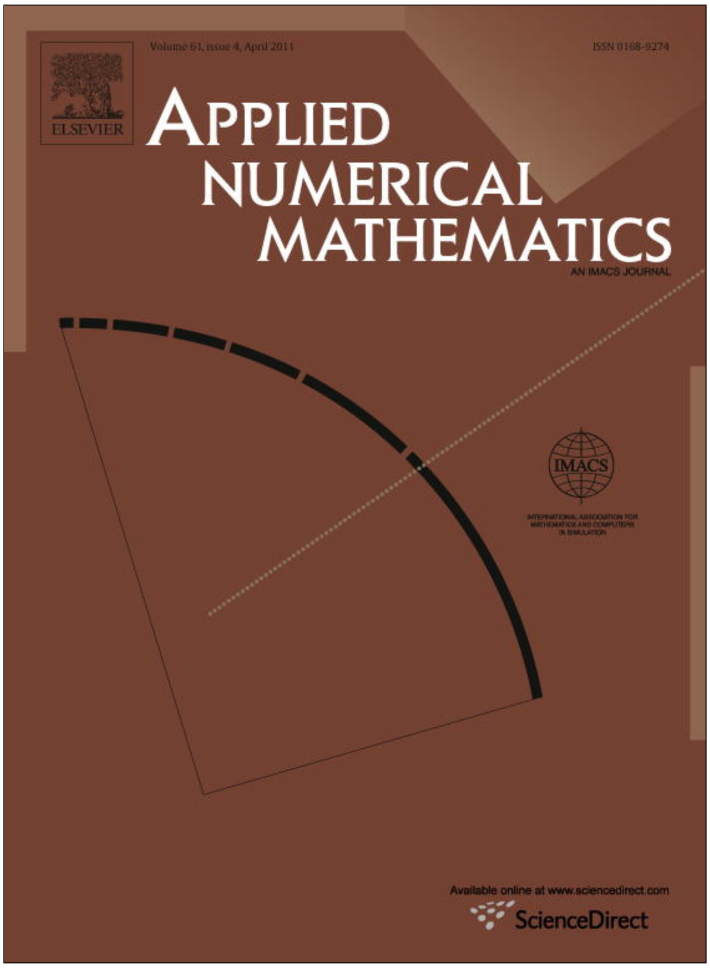
Volume 61, issue 4, April 2011
ISSN 0168-9274
ELSEVIER
APPLIED NUMERICAL MATHEMATICS
AN IMACS JOURNAL
IMACS
Available online at www.sciencedirect.com
ScienceDirect

Applied Numerical Mathematics 61 (2011) 581–592

Contents lists available at ScienceDirect

Applied Numerical Mathematics

www.elsevier.com/locate/apnum

Numerical approximation of a convolution model of $\dot{\theta}$-neuron networks

Samir Kumar Bhowmik [1]

Department of Mathematics, University of Dhaka, Dhaka, Bangladesh

A R T I C L E   I N F O

Article history:
Received 15 July 2010
Received in revised form 6 December 2010
Accepted 17 December 2010
Available online 22 December 2010

Keywords:
Neuron networks
Piecewise polynomials
Convergence

A B S T R A C T

In this article, we consider a nonlinear integro-differential equation that arises in a $\dot{\theta}$-neural networks modeling. We analyze boundedness and invertibility of the model operator, construct approximate solutions using piecewise polynomials in space, and estimate the theoretical convergence rate of such spatial approximations. We present some numerical experimental results to demonstrate the scheme.

1. Introduction

Modeling scientific problems using convolution integrals and spatial approximations of such models are of ongoing interest [3,7,10,6,5,8,19,20]. We consider such a nonlinear integro-differential equation model of transmission line in neural networks with "$\dot{\theta}$-synapses" during bursting activity [18]:

$$\frac{\partial\theta(x,t)}{\partial t} = \varepsilon \int_{\Omega} J^{\infty}(x-y)\frac{\partial\theta(y,t)}{\partial t}\,dy + f\big(\theta(x,t)\big) \tag{1}$$

with initial function $\theta(x,0) = \theta_0(x)$ where $x \in \Omega \subseteq \mathbb{R}$, $t \geqslant 0$, the angle function $\theta(x,t)$ represents the phase of the signal associated with a neuron at (x,t), f is a smooth function that represents potential effects and external inputs, J^{∞} is a kernel function and $\varepsilon > 0$ is the parameter of the model. Eq. (1) is inhibitory when $J^{\infty} < 0$ and excitatory when $J^{\infty} \geqslant 0$ that influence the neighboring neurons. For this article, we consider a nonnegative normalized kernel function i.e.,

$$J^{\infty}(x) \geqslant 0$$

and

$$\int_{\Omega} J^{\infty}(x)\,dx = 1.$$

For a neuron at position x, the angle function θ represents the phase of the signal at a time t. It is to be noted that the problem (1) is the continuous analogue of a discrete model of transmission line in neural networks with "$\dot{\theta}$-synapses" during

E-mail address: Bhowmiksk@gmail.com.

[1] The author is thankful to Professor Dugald B. Duncan, Professor Rob Stevenson and Professor Sajeda Banu for their valuable suggestions and advice. The author would also like to thank Professor Gabriel J. Lord for introducing him the model. The research was funded partially by the MACS studentship, Heriot–Watt University, UK and partially by the Netherlands Organization for Scientific Research through a VIDI grant No. 639.032.509. The author is thankful to the anonymous referees for their scrutiny.

0168-9274/$30.00 © 2010 IMACS. Published by Elsevier B.V. All rights reserved.
doi:10.1016/j.apnum.2010.12.003

sustained bursting activity [17,19]. Various properties of this type of models and their solutions have been well presented in [17].

Now if we consider a normalized kernel and $\Omega = \mathbb{R}$, then (1) can be written as

$$\left(\mathscr{L}\frac{\partial}{\partial t}\theta(\cdot,t)\right)(x) = f\big(\theta(x,t)\big) \tag{2}$$

where

$$(\mathscr{L}\psi)(x) = \int_{\Omega} J^{\infty}(x-y)\big(\psi(x) - \varepsilon\psi(y)\big)\,dy.$$

In most articles

$$f(t,\theta) = a(t) \pm \cos(\theta)$$

has been considered as a nonlinearity. Here $\theta \to \cos^{-1} a(t)$ as $t \to \infty$ for all $0 \leqslant a(t) \leqslant 1$ which stabilizes the output, and $\theta \to \infty$ when $a(t) > 1$ which oscillates the output [17, page xvi]. A saddle node bifurcation occurs when $a(t)$ increases or decreases through the value $a(t) = 1$. One may observe such phenomenon of solutions in Section 5. In this article we consider (see [18,19] for physical explanation of such choices of $f(\theta)$)

$$a(t) = \begin{cases} 2, & \text{if } t \leqslant 10, \\ 1, & \text{otherwise.} \end{cases}$$

It is well understood from the studies [19] that $\varepsilon < 1$ can be an excitatory parameter and the Gaussian kernels are associated to its bidirectional influence. So we are interested in using a normalized Gaussian kernel function

$$J^{\infty}(x) = \sqrt{\frac{\gamma}{\pi}}\exp\big(-\gamma x^2\big), \tag{3}$$

where $\gamma > 0$, $x \in \Omega$ and $0 \leqslant \varepsilon < 1$. Now the problem with a kernel of type

$$J^{\infty}(x) = \begin{cases} \sqrt{\frac{\gamma}{\pi}}\exp(-\gamma x^2), & \text{when } x \geqslant 0, \\ 0, & \text{otherwise,} \end{cases}$$

where $\gamma > 0$, corresponds to unidirectional connectivity. In both cases the influence is stronger between neurons that are close to each other. Thus Eq. (2) describes a one-dimensional chain of single neurons interacting with each other where the interaction depends on the choices of the kernel function $J^{\infty}(x)$.

Spatial approximation of this type of convolution models are interesting as well as challenging. The unknown function under the integral sign and the nonlinearity involved in the model make the approximation more challenging. The model contains a convolutional kernel. As a result the discrete analogue of the operator (matrix) becomes dense which is difficult to handle when one considers a fine grid. For a multidimensional domain it costs huge storage and computational time. There are many ways of handling such problems. In most cases scientists use some lower order schemes (with midpoint quadrature rules for integration [4,15]) to serve their purpose. Thus there is much room for improvements and we find an interest of presenting and analyzing a higher order technique for space integration.

In [15], Duncan et al. consider a phase transition model of convolution type. The authors analyze coarsening of solutions. They approximate the model using piecewise constant basis functions for space approximations. The authors also investigate the time long dynamics of solutions. A fully discrete approximation of the same model and efficiency of various linear system solvers for the resulting nonlinear system has been studied in [5]. Stability analysis of some numerical approximations of a perturbed diffusion model can be found in [8]. In [7,10,6] the authors consider a linear convolutional model. They approximate the model using a one step scheme. Then the authors investigate stability, accuracy and convergence of the scheme in detail.

Our study is motivated by [9]. In [9], the authors study numerical approximation of a nonlocal, partly nonlinear, phase transitions model. They analyze and approximate the problem using various schemes, being a finite difference method, finite element methods with collocation and the Galerkin approach (using piecewise Lagrange polynomials to form finite element basis functions), the Legendre and Tchebychef spectral methods in space followed by implicit schemes for the time integration. The authors demonstrate some numerical solutions as well as the computational error. They also estimate the theoretical errors of finite difference approximations and finite element approximations.

In [18,19], Jackiewicz et al. consider the model (1). They use the forward Euler method for time integration to form the resulting model as an integral of Fredholm type. Then the authors approximate the resulting problem using various spectral collocation methods. They present some numerical results to demonstrate their schemes. The motivation was to use global polynomials to approximate $\theta(\cdot,t)$. Solutions converge fast in such approximations if one considers smooth initial condition as well as smooth boundaries [25]. Whereas for piecewise polynomial approximations such restrictions are not needed for convergence. Also no theoretical error analysis has been done in the studies [18,19]. Thus we find an interest to approximate the problem using piecewise basis functions for spatial approximation and to analyze the error in any such approximation.

Now if we consider a spatially one-periodic initial function $\theta(x,0)$, then for all $x \in \mathbb{R}$ and $t \in \mathbb{R}_+$

$$\theta(x,t) = \theta(x+1,t).$$

Then (2) can be written as

$$\left(\mathscr{L}\frac{\partial}{\partial t}\theta(\cdot,t)\right)(x) = f\big(\theta(x,t)\big) \tag{4}$$

where

$$(\mathscr{L}\psi)(x) = \int_0^1 J(x-y)\big(\psi(x) - \varepsilon\psi(y)\big)\,dy,$$

with

$$J(x) = \sum_{r=-\infty}^{\infty} J^{\infty}(x-r)$$

for all $x \in [0,1]$. We are interested to consider the periodic domain $\Omega = [0,1]$ for spatial approximations of the model.

However, it is well understood from [14] that an integro-differential equation of type (2) defined in the infinite domain can be defined in a truncated finite domain $[A,B]$ where A and B depend on the decay of the kernel function $J^{\infty}(x)$. A closed form formula to find suitable A and B is well presented in [14]. Thus the analysis and the approximation we present here in a periodic spatial interval $\Omega = [0,1]$ can also be applied to any bounded interval $[A,B]$.

In this study, we consider the model (4) with a Gaussian kernel defined by (3) and $0 < \varepsilon < 1$. We organize the article in the following way. Boundedness and invertibility of $\mathscr{L}$ are presented in Section 2. In Section 3, we present the approximation of the problem using piecewise polynomials in space. We analyze the accuracy of the spatial approximation with the exact Galerkin inner product, as well as with quadrature on each of the Galerkin inner products assuming the solutions being smooth enough over the whole domain in Section 4. We conclude this study in Section 5 presenting some numerical results and discussions.

2. Preliminary results on $\mathscr{L}$

Here we show that the operator is bounded and invertible by imposing some reasonable restrictions on the kernel function. We need the following result to bound the operator $\mathscr{L}$.

Lemma 1. *(See [4].) Assume that*

H1 $J(x) \geqslant 0$,
H2 $J(x) = J(1-x)$,
H3 $\int_0^1 J(x)\,dx = 1$,

then for any $k \in \mathbb{Z}$, the following inequality holds

$$0 \leqslant \hat{J}_0 - \hat{J}_k \leqslant 2.$$

Proof. The proof follows from the properties of $J(x)$. □

Theorem 1. *(Similar to [4].) If $J \in L_2(\Omega)$, and satisfies* **H1–H3**, *then $\mathscr{L} : L_2(\Omega) \to L_2(\Omega)$ is bounded and*

$$\|\mathscr{L}\| \leqslant 1 + \varepsilon.$$

Proof. Applying the Fourier series expansions and the convolutional property of the Fourier transform to any ψ, $J \in L_2(\Omega)$, we get

$$\begin{aligned}(\mathscr{L}\psi)(x) &= \sum_j \hat{\psi}_j e^{2\pi ijx} - \varepsilon \sum_j \hat{\psi}_j \hat{J}_j e^{2\pi ijx} \\ &= \sum_j \hat{q}_j \hat{\psi}_j e^{2\pi ijx},\end{aligned}$$

where $\hat{q}_j = (\hat{J}_0 - \varepsilon \hat{J}_j)$. Here

$$|\hat{J}_j| = \left| \int_0^1 J(x) e^{-2\pi ijx}\, dx \right| \leqslant \int_0^1 J(x)\, dx \leqslant 1.$$

Thus applying Lemma 1 and Parseval's relation we get

$$\|\mathscr{L}\| := \sup_{\psi \neq 0} \frac{\|\mathscr{L}\psi\|}{\|\psi\|} \leqslant \max_j |\hat{J}_0 - \varepsilon \hat{J}_j| \leqslant \max_j \big(|\hat{J}_0| + \varepsilon |\hat{J}_j|\big) \leqslant 1 + \varepsilon. \qquad \square$$

Theorem 2. *If the kernel function $J(x) \in L_2(\Omega)$ satisfies the conditions* **H1–H3**, *then*

$$0 < \delta \leqslant (\hat{J}_0 - \varepsilon \hat{J}_j) \leqslant 1 + \varepsilon,$$

for all $j \in \mathbb{Z}$ and $0 < \varepsilon < 1$ where $\delta = (\hat{J}_0 - \varepsilon \sup_j |\hat{J}_j|)$ and $\sup_j |\hat{J}_j| = \hat{J}_0$.

Proof. The proof is trivial. $\square$

Now we present the main theorem that shows the invertibility of $\mathscr{L}$.

Theorem 3. *If the kernel function $J(x) \in L_2(\Omega)$ satisfies* **H1–H3**, *then for any $\psi(x) \in L_2(\Omega)$, there exists $C_2 > C_1 > 0$ such that*

$$C_1\big(\psi(x), \psi(x)\big) \leqslant \big(\mathscr{L}\psi(x), \psi(x)\big) \leqslant C_2\big(\psi(x), \psi(x)\big). \tag{5}$$

Proof. For any $\psi(x) \in L_2(\Omega)$, using Parseval's relation

$$\big(\mathscr{L}\psi(x), \psi(x)\big) = \sum_n \big(\widehat{(\mathscr{L}\psi)}_n, \hat{\psi}_n\big) = \sum_n (\hat{q}_n \hat{\psi}_n, \hat{\psi}_n).$$

Thus applying upper and lower bounds of $\hat{q}_n$ we get

$$C_1\big(\psi(x), \psi(x)\big) \leqslant \big(\mathscr{L}\psi(x), \psi(x)\big) \leqslant C_2\big(\psi(x), \psi(x)\big). \qquad \square$$

3. Numerical approximation

For numerical approximation we consider a spatial periodic $\Omega = [0, 1]$ as the domain. Here we study the Galerkin piecewise polynomial approximations in space. This study of polynomial approximation is performed following [4,11,21,23]. For any fixed $t \geqslant 0$, we look for $\frac{\partial \theta}{\partial t}(\cdot, t) \in L_2(\Omega)$ so that it satisfies

$$\left(\mathscr{L}\left(\frac{\partial \theta}{\partial t}(\cdot, t)\right) - f\big(\theta(\cdot, t)\big), v\right) = 0, \quad \forall v \in L_2(\Omega). \tag{6}$$

To approximate the solution of (6), using piecewise polynomials in space, we define N space mesh points with step size $h = \frac{1}{N}$, $x_j = jh$ for all $j = 0, 1, \ldots, N$. We subdivide Ω into N pieces $\Omega_i = [x_i, x_{i+1}]$ so that $\Omega = \bigcup_i \Omega_i$. We use the Lagrange polynomials of degree $m > 0$ in each subinterval as the basis for the spatial approximation. In each subinterval, two different choices of interpolation and quadrature points have been considered (Gauss quadrature points and Gauss–Lobatto quadrature points). To define the interpolating polynomials, we subdivide intervals Ω_i into m^* pieces and define m^* (or $m^* + 1$) points as interpolation points $x_i < x_i^j < x_{i+1}$ (or $x_i \leqslant x_i^j \leqslant x_{i+1}$, depending on quadrature and interpolation points considered). We organize the spatial points x_i^j as

$$\underline{x} = [x_1, \ldots, x_{mN}]^T$$

with

$$m = \begin{cases} m^*, & \text{for Gauss quadrature/interpolation points,} \\ m^* + 1, & \text{for Gauss–Lobatto quadrature/interpolation points.} \end{cases}$$

We define the spatial approximate solutions $\theta_h(\cdot, t) \in L_2(\Omega)$ as

$$\theta_h(x, t) = \sum_{k=1}^{N} \sum_{q=1}^{m} \theta_k^q(t) l_{m,q,k}(x) \tag{7}$$

with

$$l_{m,q,k}(x) = \begin{cases} l_{m,q,k}(x), & x \in \Omega_k, \\ 0, & \text{otherwise}, \end{cases}$$

and $\theta_k^q(t) \in \mathbb{R}$ where $l_{m,q,k}(x)$ are qth Lagrange polynomials of degree less than or equal to m. Following the standard Galerkin approach we let $\bar{\bar{\theta}}_h(\cdot,t) \in S_h$ (we consider S_h as a space of piecewise polynomials of degree less than k for some $k \geqslant 2$ in Ω), to satisfy

$$\left(\mathscr{L}\frac{\partial \bar{\bar{\theta}}_h}{\partial t}(x,t) - f\big(\bar{\bar{\theta}}_h(x,t)\big), l_{m,q,k}(x)\right) = 0 \tag{8}$$

for all m, q, k and we consider the approximate solutions $\bar{\theta}_h(\cdot,t) \in S_h$ to satisfy

$$\left(\mathscr{L}\frac{\partial \bar{\theta}_h}{\partial t}(x,t) - f_h\big(\bar{\theta}_h(x,t)\big), l_{m,q,k}(x)\right) = 0. \tag{9}$$

Here f_h is defined by using the product approximation [13,24]

$$\big(f_h(\theta_h)\big)(x) = I_h f\left(\sum_{j=1}^{N}\sum_{q=1}^{m}\theta_j^q l_{m,q,j}(x)\right) \approx \sum_{j=1}^{N}\sum_{q=1}^{m} f\big(\theta_j^q\big) l_{m,q,j}(x), \tag{10}$$

where

$$\sum_{j=1}^{N}\sum_{q=1}^{m} f\big(\theta_j^q\big) l_{m,q,j}(x)$$

is the unique element in the solution space which interpolates

$$f\left(\sum_{j=1}^{N}\sum_{q=1}^{m}\theta_j^q l_{m,q,j}(x)\right)$$

at the nodes x_i and I_h is the interpolation operator.

Before further discussion of discretization we define the discrete inner product and the discrete norm in the following way:

Consider the interval $[a,b]$. For any two functions w and g, we consider the discrete inner product $(w,g)_h$ by [9]

$$(w,g)_h = \sum_{j=1}^{N}\sum_{k=1}^{m}\mu_j^k w\big(x_j^k\big) g\big(x_j^k\big) \tag{11}$$

where N is the number of subintervals of $[a,b]$, m is the number of quadrature points used in each subinterval, x_j^k are the quadrature points and $\mu_j^k > 0$ are quadrature weights (we have considered the Gauss or the Gauss–Lobatto quadrature weights). We also define the discrete analogue of the continuous L_2 norm by

$$\|w\|_h^2 = (w,w)_h. \tag{12}$$

Considering a numerical integration scheme with nonzero quadrature weights, and using Lagrange polynomials for interpolation, we approximate (9) as

$$\begin{aligned} &\left(\mathscr{L}\frac{\partial \theta_h}{\partial t}(x,t), l_{m,q,p}(x)\right)_h - \big(f_h, l_{m,q,p}(x)\big)_h \\ &\quad = \sum_{q=1}^{m}\mu_p^q\left[\mathscr{L}\frac{\partial \theta_h}{\partial t}\big(x_p^q,t\big) l_{m,q,p}\big(x_p^q\big) - \big(f_h(\theta_h)\big)\big(x_p^q,t\big) l_{m,q,p}\big(x_p^q\big)\right] = 0, \end{aligned} \tag{13}$$

for all $p = 1,\ldots,N$. Now using the inner product $(\mathscr{L}\frac{\partial\theta_h}{\partial t}(x,t), l_{m,q,p}(x))_h$ with some quadrature rule with nonzero weights it is easy to verify that the operator acting on (13) is positive definite (see [4] for similar discussion) if $0 < \varepsilon < 1$. Thus the time dependent system of ordinary differential equations

$$\left(\mathscr{L}\frac{\partial \theta_h}{\partial t}(x,t), l_{m,q,p}(x)\right)_h - \big(f_h, l_{m,q,p}(x)\big)_h = 0, \tag{14}$$

for all $p = 1,2,\ldots,N$, has a unique solution for all $0 < \varepsilon < 1$.

4. Error estimate

In this section we discuss convergence analysis of the Galerkin finite element approximation based on piecewise polynomials in space used to solve Eq. (4). Before we go into the main discussion we introduce the following definition:

We define the Sobolev spaces H^k through the derivatives as

$$H^k(\Omega) = \left\{\psi\colon \frac{d^r\psi}{dx^r} \in L_2(\Omega),\ \text{for all } 0 \leqslant r \leqslant k\right\},$$

and the standard norm of such space can be defined as

$$\|\psi\|_{H^k} = \sqrt{\sum_{0\leqslant r\leqslant k} \left\|\frac{d^r\psi}{dx^r}\right\|_{L_2}^2}.$$

Sometimes the norm $\|\cdot\|_{H^k}$ is also denoted by $\|\cdot\|_k$. When $k=0$, the H^k norm becomes the L_2 norm and we denote the L_2 norm by $\|\cdot\|$.

We let $\theta \in L_2(\Omega)$ to satisfy

$$\left(\mathscr{L}\frac{\partial\theta}{\partial t}(\cdot,t), v\right) - \big(f\big(\theta(\cdot,t)\big), v\big) = 0, \quad \text{for all } v \in L_2(\Omega). \tag{15}$$

Here we assume that θ_0 and θ are sufficiently smooth (considering $\theta(\cdot,t) \in H^k(\Omega)$, $t \geqslant 0$, $k > 1$) for this analysis. Here c, c_i, C, and C_i denote positive constants, not necessarily the same in different occasions. We assume $S = H^k(\Omega)$ for some $k > 1$. It is also assumed that the solutions $\theta(\cdot,t) \in S$ which is required for the error analysis.

4.1. Exact Galerkin inner product approximation

Let $S_h \subset S$ be a finite-dimensional subspace that contains approximate solutions $\theta_h(x,t)$ using piecewise polynomials of degree at most $k-1$. Let P be a projection operator from the space S onto its subspace S_h. That is, $v \in S$ implies that $Pv \in S_h$ and it satisfies

$$(\theta - P\theta, v_h) = 0 \quad \text{for all } v_h \in S_h, \tag{16}$$

so that $P\theta$ is the L_2 best fit to θ. It is observed [23] that

$$\|\theta - \theta_I\| \leqslant Ch^{r+1}\|\theta\|_{r+1}, \quad \text{where } 1 \leqslant r < k,$$

for any $\theta \in H^{r+1}$ where I stands for interpolation by piecewise polynomials of degree $k-1$. Since $P\theta$ is the L_2 best fit to θ from S_h, from [22] it follows that

$$\|\theta - P\theta\| \leqslant \|\theta - \theta_I\| \leqslant Ch^{r+1}\|\theta\|_{r+1}, \quad 1 \leqslant r < k, \tag{17}$$

for all such interpolants $\theta_I \in S_h$. It is to be noted that r are referred to as the order of accuracy in our spatial piecewise polynomial approximation in this article.

The approximate solution $\theta_h(\cdot,t) \in S_h$ satisfies

$$\left(\mathscr{L}\frac{\partial\theta_h}{\partial t}(\cdot,t) - f_h\big(\theta_h(\cdot,t)\big), v_h\right) = 0 \quad \text{for all } v_h \in S_h. \tag{18}$$

From (18) and (15)

$$\left(\mathscr{L}\left(\frac{\partial\theta}{\partial t}(x,t) - \frac{\partial\theta_h}{\partial t}(x,t)\right), v_h\right) - \big(f(\theta) - f_h(\theta_h), v_h\big) = 0. \tag{19}$$

Let $e = \frac{\partial\theta}{\partial t} - \frac{\partial\theta_h}{\partial t}$ be the error in the spatial finite element approximation and we write

$$e = \frac{\partial\theta}{\partial t} - \frac{\partial\theta_h}{\partial t} = \frac{\partial\theta}{\partial t} - \frac{\partial P\theta}{\partial t} + \frac{\partial P\theta}{\partial t} - \frac{\partial\theta_h}{\partial t}. \tag{20}$$

Let

$$\phi = \frac{\partial(P\theta - \theta_h)}{\partial t} \in S_h \tag{21}$$

which will be needed in the later part of this section (it is to be noted that $\frac{\partial\theta}{\partial t}$ is also denoted by θ_t). Now we need the following result to support the analysis in this section.

Proposition 4.1. *If $f(\theta(\cdot,t))$ is a smooth function in Ω for all $\theta \in S$, $f_h(\theta_h(\cdot,t))$ is defined by (10), and $f(\theta_h) \in H^{r+1}(\Omega_j)$ for all $j = 1, 2, \dots, N$, then*

$$\left\| f(\theta) - f_h(\theta_h) \right\| \leqslant C_2 h^{r+1} + C_3 h^{r+1} \|\theta\|_{r+1}, \tag{22}$$

for some constants $C_2 > 0$ and $C_3 > 0$ and $1 \leqslant r < k$, if θ, and hence $f'(\theta)$ is bounded for all $t \in [0, T]$ for some finite $T \geqslant 0$.

Proof. The proof follows from [4]. □

The main result of this section is represented by the following error estimate.

Theorem 4. *If $\theta_h(\cdot,t) \in S_h$ satisfies (18), and $\theta(\cdot,t) \in S$ satisfies (15), $\frac{\partial}{\partial t}\theta(\cdot,t) \in H^k$ then the following inequality holds*

$$\left\| \frac{\partial \theta(\cdot,t)}{\partial t} - \frac{\partial \theta_h(\cdot,t)}{\partial t} \right\| \leqslant C h^{r+1}, \quad \text{for } 1 \leqslant r < k \text{ and } C > 0.$$

Proof. Here

$$\|e\| \leqslant \left\| \frac{\partial \theta}{\partial t} - \frac{\partial (P\theta)}{\partial t} \right\| + \left\| \frac{\partial (P\theta)}{\partial t} - \frac{\partial \theta_h}{\partial t} \right\|.$$

(19) can be written as

$$\left(\mathscr{L}\left(\frac{\partial \theta}{\partial t} - \frac{\partial (P\theta)}{\partial t} \right), v_h \right) + \left(\mathscr{L}\left(\frac{\partial (P\theta)}{\partial t} - \frac{\partial \theta_h}{\partial t} \right), v_h \right) - \left(f(\theta) - f_h(\theta_h), v_h \right) = 0, \tag{23}$$

for all $v_h \in S_h$. Thus it remains to prove

$$\|\phi\| \leqslant C h^{r+1}, \quad \text{for } 1 \leqslant r < k,$$

since from (17) it follows that

$$\left\| \frac{\partial \theta(\cdot,t)}{\partial t} - \frac{\partial (P\theta)(\cdot,t)}{\partial t} \right\| \leqslant C h^{r+1}, \quad \text{for } 1 \leqslant r < k,$$

assuming $\frac{\partial \theta(\cdot,t)}{\partial t} \in H^{r+1}$. Replacing v_h by ϕ in (23) we get

$$\left| (\mathscr{L}\phi, \phi) \right| \leqslant \left| \left(\mathscr{L} \frac{\partial (P\theta - \theta)}{\partial t}, \phi \right) \right| + \left| \left(f(\theta) - f_h(\theta_h), \phi \right) \right|. \tag{24}$$

Now to find an upper bound of $\|e\|$ we need to find norm of three terms of (24). For the first part of the RHS of (24) we have

$$\begin{aligned} \left| \left(\mathscr{L} \frac{\partial (\theta - P\theta)}{\partial t}, \phi \right) \right| &\leqslant \|\mathscr{L}\| \left\| \frac{\partial (\theta - P\theta)}{\partial t} \right\| \|\phi\| \\ &\leqslant C \left\| \frac{\partial (\theta - P\theta)}{\partial t} \right\| \|\phi\| \end{aligned} \tag{25}$$

where $C > 0$, second part of the RHS gives

$$\left| \left(f(\theta) - f_h(\theta_h), \phi \right) \right| \leqslant \left\| f(\theta) - f_h(\theta_h) \right\| \|\phi\|. \tag{26}$$

Now from (5) one gets

$$C_1(\phi, \phi) \leqslant (\mathscr{L}\phi, \phi), \quad \text{for some } C_1 > 0. \tag{27}$$

So

$$\|\phi\| \leqslant \left\| \frac{\partial}{\partial} (\theta - P\theta) \right\| + \left\| f(\theta) - f_h(\theta_h) \right\|. \tag{28}$$

Thus applying (17) and (25) in (28), and then canceling common terms we get

$$C_1 \|\phi\| \leqslant C_4 h^{r+1} \left\| \frac{\partial \theta}{\partial t} \right\|_{r+1} + \left\| f(\theta) - f_h(\theta_h) \right\|, \quad \text{for } 1 \leqslant r < k, \tag{29}$$

for some $C_1 > 0$, and $C_4 > 0$. Combining (22) and (29) we get the required bound

$$\left\| \phi(t) \right\| \leqslant C_2^* h^{r+1}, \quad \text{for } 1 \leqslant r < k,$$

for some $C_2^* > 0$, which proves our claim. □

4.2. Quadrature Galerkin approximation

It is a practice as well as obvious that the integrals are approximated by quadrature rules unless they happen to be easy to calculate exactly. There are several standard rules to serve the purpose. We use the Gauss/Gauss–Lobatto quadrature (the so-called mass lumped technique) to serve our purpose and show that there is no loss of accuracy if one uses such an alternative.

Here we analyze the convergence of the Galerkin method with quadrature on inner product integrals (Gauss/Gauss–Lobatto quadrature (the so-called mass lumped technique) [23]). From [1,2,12,16] and many references therein it is well understood that

$$\|\cdot\|_h \equiv \|\cdot\|$$

for all functions in the approximation space S_h, i.e., there exist $C_1 > 0, C_2 > 0$ such that

$$C_1\|v_h\| \leqslant \|v_h\|_h \leqslant C_2\|v_h\|, \quad \text{for all } v_h \in S_h. \tag{30}$$

Here we consider $\theta_h(\cdot,t) \in S_h$ as the solution of the quadrature approximation of (18)

$$\left(\mathscr{L}\left(\frac{\partial\theta_h(\cdot,t)}{\partial t}\right)(x), v_h\right)_h = \left(f_h\left(\theta_h(x,t)\right), v_h\right)_h, \quad \text{for all } v_h \in S_h \tag{31}$$

where

$$\left(\mathscr{L}\psi(x), v\right)_h = \sum_{i,j=1}^{n}\sum_{r_1,r_2=1}^{m} \mu_i^{r_1}\mu_j^{r_2} J\left(x_i^{r_1} - x_j^{r_2}\right)\left(\psi\left(x_j^{r_2}\right) - \varepsilon\psi\left(x_i^{r_1}\right)\right)v\left(x_i^{r_1}\right). \tag{32}$$

This analysis is performed following [4,9]. We define the projection operator P_h such that $v \in S$ implies $P_h v \in S_h$, and satisfies [4,9]

$$(\theta - P_h\theta, v)_h = 0,$$

for all $v \in S_h$ (so that $P_h\theta$ is the L_2 best fit of θ in this discrete norm). Combining (17) and (30)

$$\|\theta - P_h\theta\|_h \leqslant \|\theta - \theta_I\|_h \leqslant C\|\theta - \theta_I\| \leqslant C_Q h^{r+1}\|\theta\|_{r+1}, \quad \text{for } 1 \leqslant r < k, \tag{33}$$

where the interpolant $\theta_I \in S_h$. Now we find the error bound in the Galerkin method with a quadrature approximation for space integrals by the following result.

Theorem 5. *If $\theta_h \in S_h$ satisfies* (31)*, and $\theta \in S$ satisfies* (15)*, $\frac{\partial}{\partial t}\theta(\cdot,t) \in H^k$, then the following inequality holds*

$$\|e\|_h = \left\|\frac{\partial\theta}{\partial t} - \frac{\partial\theta_h}{\partial t}\right\|_h \leqslant C^Q h^{r+1},$$

for $1 \leqslant r < k$ and $C^Q > 0$ depends on the quadrature rule used.

Proof. Following a similar process to that of the Galerkin method with exact integration (20) can be written as

$$\left\|\frac{\partial(\theta - \theta_h)}{\partial t}\right\|_h \leqslant \left\|\frac{\partial(\theta - P_h\theta)}{\partial t}\right\|_h + \left\|\frac{\partial(P_h\theta - \theta_h)}{\partial t}\right\|_h. \tag{34}$$

Similar to (23) the quadrature error can be presented as [9]

$$\left(\mathscr{L}\frac{\partial(\theta - P_h\theta)}{\partial t}, v_h\right)_h + \left(\mathscr{L}\frac{\partial(P_h\theta - \theta_h)}{\partial t}, v_h\right)_h - \left(f(\theta) - f_h(\theta_h), v_h\right)_h = 0, \tag{35}$$

for all $v_h \in S_h$. Now (35) can be rearranged as

$$\left(\mathscr{L}\frac{\partial(P_h\theta - \theta_h)}{\partial t}, v_h\right)_h = \left(\mathscr{L}\frac{\partial(-\theta + P_h\theta)}{\partial t}, v_h\right)_h + \left(f(\theta) - f_h(\theta_h), v_h\right)_h \tag{36}$$

for all $v_h \in S_h$. Considering

$$\phi_h = \frac{\partial(P_h\theta - \theta_h)}{\partial t} \in S_h$$

and replacing v_h by ϕ_h, (36) can be written as

$$\left|(\mathscr{L}\phi_h,\phi_h)_h\right| \leqslant \left|\left(\mathscr{L}\frac{\partial(-\theta+P_h\theta)}{\partial t},\phi_h\right)_h\right| + \left|\big(f(\theta)-f_h(\theta_h),\phi_h\big)_h\right|. \tag{37}$$

Now

$$\left|\big(f(\theta)-f_h(\theta_h),\phi_h\big)_h\right| \leqslant \|f-f_h\|_h\|\phi_h\|_h.$$

Following [4,9] (similar to the exact inner product estimate)

$$\big\|f(\theta)-f_h(\theta_h)\big\|_h \leqslant C_Q^1 h^{r+1}\|\theta\|_{r+1} + C_Q^2 h^{r+1} \tag{38}$$

for all $1 \leqslant r < k$ if θ, and hence $f'(\theta)$, is bounded for all $t \in [0,T]$ ($T \geqslant 0$ is a finite number) C_Q^i, $i=1,2$ are constants depend on the quadrature rule used. Now applying (33) we get

$$\begin{aligned}\left|\left(\mathscr{L}\frac{\partial(\theta-P_h\theta)}{\partial t},\phi_h\right)_h\right| &\leqslant C_Q^*\left\|\frac{\partial(\theta-P_h\theta)}{\partial t}\right\|_h\|\phi_h\|_h\\ &\leqslant C_Q h^{r+1}\left\|\frac{\partial\theta}{\partial t}\right\|_{r+1}\|\phi_h\|_h,\end{aligned} \tag{39}$$

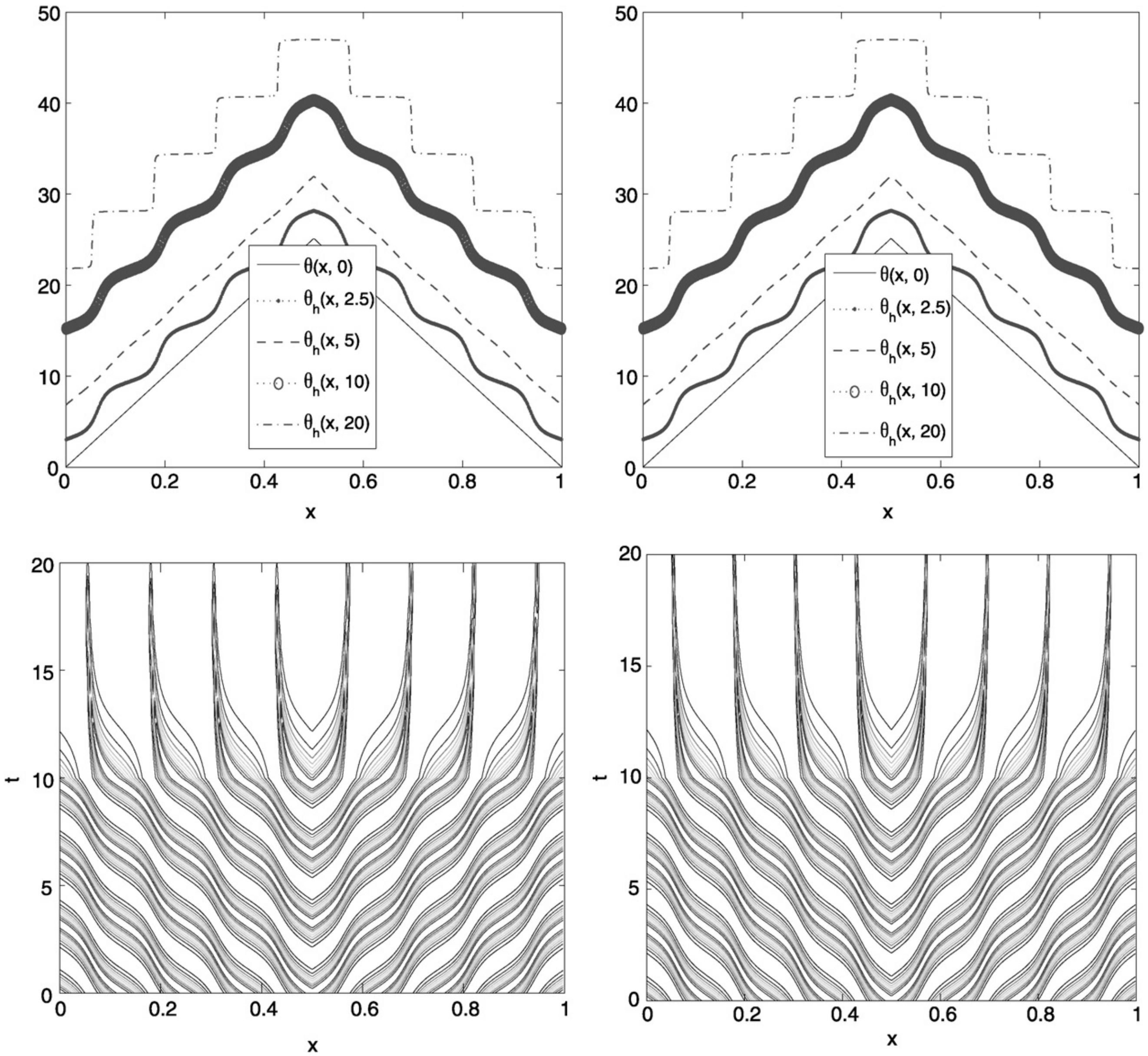

Fig. 1. Here $f(\theta) = a + \cos(\theta)$ where $a = 2$ if $t \leqslant 10$ and $a = 1$ if $\theta > 10$ and $\varepsilon = 0.1$. We present contours at grid values $\cos(\theta_h(\cdot,t))$ (lower two plots) and $\theta_h(\cdot,t)$ (upper two plots) at grid points with various choices of polynomial approximations where $\theta_0(x,0) = 16\pi x$ when $0 \leqslant x \leqslant 0.5$ and $\theta_0(x,0) = 16\pi(1-x)$ when $0.5 < x \leqslant 1$ (P_1 (left figures) and P_2 (right figures) polynomial approximations with 2^8 space elements).

where $1 \leqslant r < k$ and $C_Q > 0$ is a constant depends on quadrature used and $\frac{\partial}{\partial t}\theta(\cdot,t) \in H^{r+1}$. Similar to the exact Galerkin inner product approximation, a discrete version of (5) can be written as

$$C_Q^1 \left|(\phi_h, \phi_h)_h\right| \leqslant \left|(\mathscr{L}\phi_h, \phi_h)_h\right|. \tag{40}$$

Thus combining inequalities (38), (39), and (40), Eq. (37) can be written as

$$\left\|\phi_h(t)\right\|_h \leqslant C_Q^* h^{r+1}, \quad \text{for } 1 \leqslant r < k,$$

for some C_Q^* completes the proof since

$$\left\|\frac{\partial(\theta - P_h\theta)}{\partial t}\right\|_h \leqslant C_Q h^{r+1}, \quad \text{for } 1 \leqslant r < k,$$

for some $C_Q > 0$ which depends on the quadrature rule used. □

5. Numerical experiments and discussions

Here we present and discuss numerical solutions obtained from the scheme (14) defined in Section 3. The semidiscrete time dependent system of differential equations (14) is solved using MATLAB with various choices of initial functions, nonlinearity, and parameter. The kernel defined in (3) with $\gamma = 10$, and $f(t,\theta)$ defined in the introduction are considered for our numerical experiments. We use various Lagrange polynomials, the Gauss (–Lobatto) quadrature points for interpolation, and quadrature to solve the problem considering $N = 2^8$ space elements. In Figs 1, 2, and 3, we present the approximate solutions $\theta_h(\cdot,t)$ and contours of $\cos(\theta_h(\cdot,t))$ in $\Omega = [0,1]$ to observe the propagation of the initial wave (here solutions are plotted at grid points for all cases). It is observed that the P_i polynomial approximations give the same pattern of approximate solutions $\theta_h(x,t)$ (with $i = 1, 2$ only). Here we notice that the solutions from both the polynomial approximations evolve to the same steady states which are the staircases since $f(\theta) = 0$ gives $\cos(\theta) = \pm 1$ as $t \to \infty$. The number of jumps on the steady state patterns of solutions depend on the solution pattern of $\theta(\cdot,10)$ (of $\theta(\cdot,5)$ in Fig. 3). From these numerical results we notice that the solution patterns depend on the nonlinearity, and that the jumps on steady state solutions depend on the choices of initial function.

In Fig. 4, we show the computational error in such a spatial approximation with a fixed initial function, and considering $\varepsilon = 0.1$ and the error computed at $t = 1$. It is noticed that the approximations presented in Fig. 4 give the computational accuracy of order $\mathscr{O}(h^2)$ and order $\mathscr{O}(h^3)$, respectively, and these computations agree with our theoretical error estimates (presented in the previous two sections).

The above discussion implies that a numerical method based on any kth degree piecewise polynomials for spatial approximation for the $\dot{\theta}$ model is accurate of order $\mathscr{O}(h^{r+1})$, where $k > r \geqslant 1$.

Some restrictions on the model operator are imposed in this study for the theoretical error estimates as well as for computations. We consider a nonnegative kernel with some additional requirements needed for the analysis. The theoretical

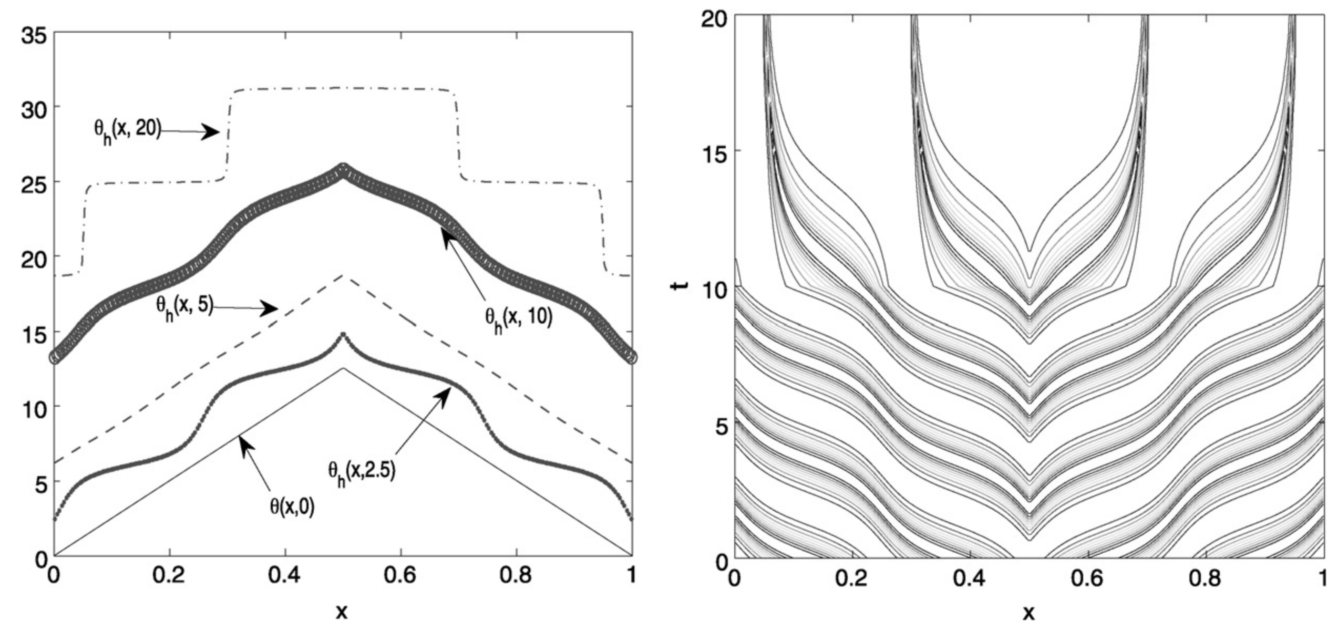

Fig. 2. We consider $f(\theta) = 2 - \cos(\theta)$ when $t \leqslant 10$ and $f(\theta) = 1 - \cos(\theta)$ when $\theta > 10$, as well as $\varepsilon = 0.001$. Contours (at grid values $\cos(\theta_h(\cdot,t))$, right plot), and $\theta_h(\cdot,t)$ (left plot) are presented where $\theta_0(x,0) = 8\pi x$ when $0 \leqslant x \leqslant 0.5$, $\theta_0(x,0) = 8\pi(1-x)$ when $0.5 < x \leqslant 1$. Solutions are computed using P_1 polynomial approximations with 2^8 space elements.

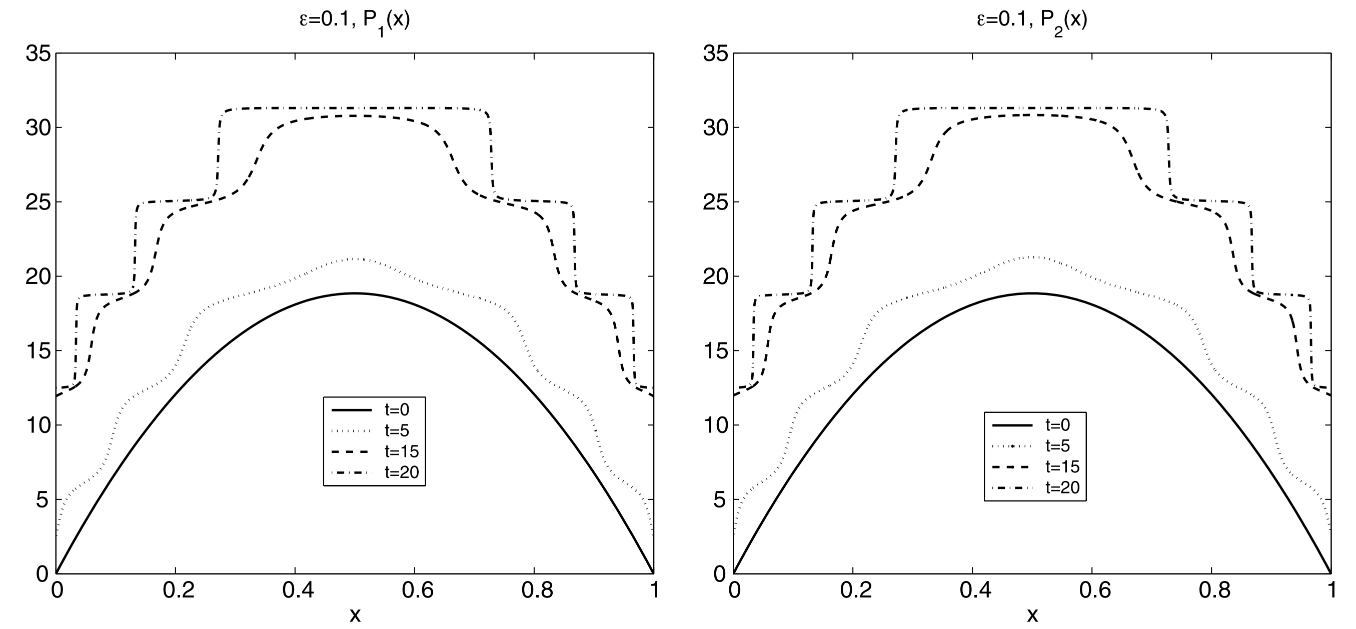

Fig. 3. We consider $f(\theta) = a - \cos(\theta)$ where $a = 2$ if $t \leqslant 5$ and $a = 1$ if $\theta > 5$ and $\varepsilon = 0.1$. $\theta_h(x, t)$ is plotted at grid points with various choices of polynomial approximations where $\theta_0(x, 0) = 24\pi x(1 - x)$ and $N = 2^8$ considering Gauss quadrature points for interpolation and integrations.

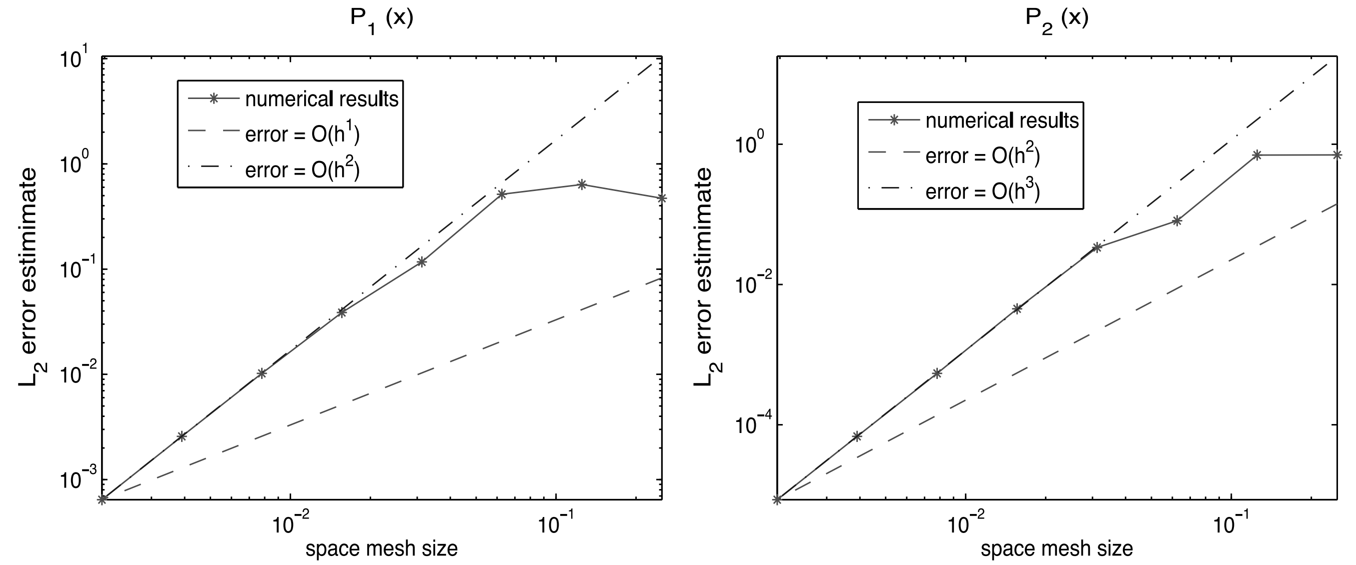

Fig. 4. Here we consider $f(\theta) = a + \cos(\theta)$ where $a = 2$ if $t \leqslant 10$ and $a = 1$ if $\theta > 10$, $\varepsilon = 0.1$, and $\theta_0 = 16\pi x$ if $0 \leqslant x \leqslant 0.5$, $\theta_0 = 16\pi(1 - x)$ if $0.5 < x \leqslant 1$. Here we compute numerical error at $t = 1$.

error analysis is performed assuming both the exact solutions and the approximate solutions are sufficiently smooth in Ω for the study. We consider a bi-directional kernel that is related to the excitatory neurons.

Few questions can be addressed as future research interest. It would be interesting to consider kernels related to inhibitory and unidirectional neurons for both computation and analysis. Moreover, one may consider multidimensional spatial domain for both approximation and analysis, which is of course more challenging to implement.

References

[1] M. Bakker, Galerkin methods for even-order parabolic equations in one space variable, SIAM Journal on Numerical Analysis 19 (3) (June 1982) 571–587.
[2] M. Bakker, One-dimensional Galerkin methods and super convergence at interior nodal points, SIAM Journal on Numerical Analysis 21 (1) (February 1984) 101–110.
[3] P.W. Bates, P.C. Fife, X. Ren, X. Wang, Travelling waves in a convolution model for phase transitions, Archive for Rational Mechanics and Analysis 138 (2) (July 1997) 105–136.
[4] S.K. Bhowmik, Numerical approximation of a nonlinear partial integro-differential equation, PhD thesis, Heriot–Watt University, Edinburgh, UK, April 2008.
[5] S.K. Bhowmik, Numerical computation of a nonlocal double obstacle problem, International Journal of Open Problems in Computer Science and Mathematics 2 (1) (March 2009) 19–36.

[6] S.K. Bhowmik, Stability and convergence analysis of a one step approximation of a linear partial integro-differential equation, Numerical Methods for Partial Differential Equations, online published, March 2010.
[7] S.K. Bhowmik, Numerical convergence of a one step approximation of an integro-differential equation, Technical Report, arXiv:1005.5344v1, May 2010.
[8] S.K. Bhowmik, Stable numerical schemes for a partly convolutional partial integro-differential equation, Applied Mathematics and Computation 217 (8) (December 2010) 4217–4226.
[9] S.K. Bhowmik, D.B. Duncan, Piecewise polynomial approximation of a nonlinear partial integro-differential equation, Technical Report, Department of Mathematics, Heriot–Watt University, December 2009.
[10] S.K. Bhowmik, D.B. Duncan, M. Grinfeld, G.J. Lord, Finite to infinite steady state solutions, bifurcations of an integro-differential equation, Technical Report, arXiv:1004.5136, April 2010, Discrete and Continuous Dynamical Systems, Series B, in press.
[11] S.C. Brenner, L.R. Scott, The Mathematical Theory of Finite Element Methods, Springer, 2002.
[12] J.H. Cerutti, S.V. Parter, Collocation methods for parabolic partial differential equations in one space dimension, Numerische Mathematik 26 (1976) 227–254.
[13] I. Christie, D.F. Griffiths, A.R. Mitchell, J.M. Sanz-Serna, Product approximation for non-linear problems in the finite element method, IMA Journal of Numerical Analysis 1 (1981) 253–266.
[14] D.J. Duffy, Finite Difference Methods for Financial Engineering: A Partial Differential Equation Approach, Wiley Finance, John Wiley and Sons, 2006.
[15] D.B. Duncan, M. Grinfeld, I. Stoleriu, Coarsening in an integro-differential model of phase transitions, European Journal of Applied Mathematics 11 (2000) 511–523.
[16] C.E. Greenwell-Yanik, G. Fairweather, Analysis of spline collocation methods for parabolic and hyperbolic problems in two space variables, IMA Journal on Numerical Analysis 23 (2) (1986) 282–296.
[17] F.C. Hoppensteadt, An Introduction to the Mathematics of Neurons: Modelling in the Frequency Domain, second ed., Cambridge University Press, New York, 1997.
[18] Z. Jackiewicz, M. Rahman, B.D. Welfert, Numerical solution of a Fredholm integro-differential equation modelling neural networks, Applied Numerical Mathematics 56 (2006) 423–532.
[19] Z. Jackiewicz, M. Rahman, B.D. Welfert, Numerical solution of a Fredholm integro-differential equation modelling $\dot{\theta}$-neural networks, Applied Mathematics and Computation 195 (2008) 523–536.
[20] C.R. Laing, W.C. Troy, PDE methods for nonlocal models, SIAM Journal on Applied Dynamical Systems 2 (3) (2003) 487–516.
[21] S. Larsson, V. Thomée, Partial Differential Equation with Numerical Methods, Springer, 2009.
[22] E. Süli, D. Mayers, An Introduction to Numerical Analysis, Cambridge University Press, 2003.
[23] V. Thomée, Galerkin Finite Element Methods for Parabolic Problems, Springer Series in Computational Mathematics, 1997.
[24] Y. Tourigny, Product approximation for nonlinear Klein–Gordon equations, IMA Journal of Numerical Analysis 9 (1990) 449–462.
[25] L.N. Trefethen, Spectral Methods in MATLAB, SIAM, 2000.